



## Li<sub>2</sub>SrTa<sub>2</sub>O<sub>7</sub> Compound: Theoretical Study of Electronic and Optical properties

Murat AYCIBIN<sup>1\*</sup> <sup>1</sup>Van YuzuncuYil University, Faculty of Science, Department of Physics, 65080, VAN, TURKEY

### Highlights

- Li<sub>2</sub>SrTa<sub>2</sub>O<sub>6</sub> belongs to Ruddlesden-Popper (RP) layered perovskite family.
- Li<sub>2</sub>SrTa<sub>2</sub>O<sub>6</sub> has wide forbidden energy band gap.
- Li<sub>2</sub>SrTa<sub>2</sub>O<sub>6</sub> is semiconductor with indirect transition for two phases.
- Optical properties depend on axes due to structural properties.
- Broad spectra of the complex dielectric function show high absorption.

### ArticleInfo

Received: 18/09/2018

Accepted: 20/06/2019

### Keywords

Electronic Structure

Li<sub>2</sub>SrTa<sub>2</sub>O<sub>7</sub>

Wien2k

Ruddlesden-Popper

Phase

### Abstract

The electronic structures and optical properties of Li<sub>2</sub>SrTa<sub>2</sub>O<sub>7</sub> belongs Ruddlesden-Popper layered perovskite family are studied by first-principles self-consistent local density calculations in its orthorhombic and tetragonal phases. The exchange-correlation potential were introduced within a framework of the generalized gradient approximation (GGA). In both phases, the conduction band minimum is at the zone center while the valance band is located at H and N high symmetry points for orthorhombic and tetragonal phases, respectively. The dynamic dielectric function, optical properties such as reflectance, refractivity and extinction coefficient for two phases are reported for energy range 0-50 eV. The variation in electronic and optical properties can be interpreted to attribute to higher symmetry, coordination number or Li, Sr and Ta atoms and packing density in tetragonal phase than in orthorhombic phase.

## 1. INTRODUCTION

Ruddlesden-Popper (RP) layered perovskite family [1] has been attracted researchers due to its exciting properties such as photocatalysts [2], ion-exchange and intercalation [3-5], ionic conductivity [6] etc... Above stated properties of RP make these type materials be good candidate in technological applications. Li<sub>2</sub>SrTa<sub>2</sub>O<sub>7</sub> (LSTO) [7] belongs to RP family. In literature, there are so limited studies related with this compound and all studies, we came cross, were performed experimentally [2, 7-9]. In these studies, researchers synthesized [7] or investigated photocatalysts properties [2], ion-exchange, intercalation, grafting [8] and phase transition [9] properties of compound. In the first time, LSTO was synthesized by Floros *et al.* [10] and Fourquet *et al.* [7]. First study devoted on LSTO to obtain structural parameters was carried out by Floros *et al.* [10]. They determined space group of LSTO as a Cmc<sub>2</sub>m and gave lattice parameters related with space group. Meanwhile, Fourquet *et al.* also performed experimental study to investigate structural parameters of LSTO [7]. They used x-ray diffraction method to perform structural analysis. According to their finding, space group of compound is I4/mmm. There is a disagreement between two studies done by Fourquet and Floros. In order to clarify situation, Crosnier-Lopez *et al.* performed complete structural study to determine compound structure via several techniques [9]. They showed that LSTO occurs in orthorhombic phase (Cmc<sub>2</sub>m at room temperature) and observed that the compound undergoes a transition to the tetragonal phase (I4/mmm at 300 °C).

In this work, the result of a detailed performance on the electronic structure and optical properties of two phases LSTO compound were reported. Intense search in literature reveals that either theoretical or

\*e-mail: murataycibin@yyu.edu.tr

experimental studies on the electronic and optical properties of LSTO have been performed. Therefore, this study will cover the lack of theoretical data and serve as a guide to researchers who like to use LSTO compound in industrial application.

## 2. COMPUTATIONAL METHOD

All the calculation were carried out using the Wien2k [11] which is embedded in the framework of Density functional Theory (DFT) and uses Linearized Augmented Plane Wave (LAPW)[12]. Before starting to compute physical properties of materials, Wien2k software requires some initial parameters to construct structural file. One way to get required parameters is to obtain them from previously performed experimental study. Therefore, the required parameters such as the atomic position, space group and lattice constants were taken from Crosnier-Lopez's work [9]. The electronic configuration of the compound is Li [He]  $2s^1$ , Sr [Kr]  $4s^2$ , Ta [Xe]  $4f^{14} 5d^3 6s^2$  and O [He]  $2s^2 2p^4$ .

After constructed structure file for Wien2k, initial calculation was run. For this aim, the cut of energy, which is the separation between valence band and conduction band, was set to - 9 Ry energy value and 648 high symmetry k points were generated in  $17 \times 17 \times 16$  grid for the density in Brillion zone (BZ). There are four embedded potentials to be used for exchange-correlation effect in Wien2k namely the local spin density approximation(LSDA)[13], the generalized gradient approximation (GGA) using the Perdew-Burke-Ernzerhof[14], WC-GGA [15, 16] and PBEsol-GGA [17]. After all the parameters were obtained, physical properties of compound can be calculated.

## 3. RESULT & DISCUSSION

### 3.1. Structural Properties

LSTO is in orthorhombic phase with space group Cmcm at Room Temperature (RT) and tetragonal phase with space group I4/mmm at 300 °C. The necessity compound structural information (lattice parameters, space groups and atomic position) was taken from Crosnier-Lopez's paper [9]. The volume-energy optimization process was run to obtain theoretical lattice constants to determine suitable potential embedded in Wien2k for exchange-correlation potential. Then, the Birch-Murnaghan equation of state [18, 19] was used for fitting purpose to obtain theoretical values of the lattice constant. The obtained theoretical lattice constants depending on selected potential were inserted in Table-1. According to obtained results, PBE-GGA gave best lattice constants which are the closest to experimental values (Figure 1).

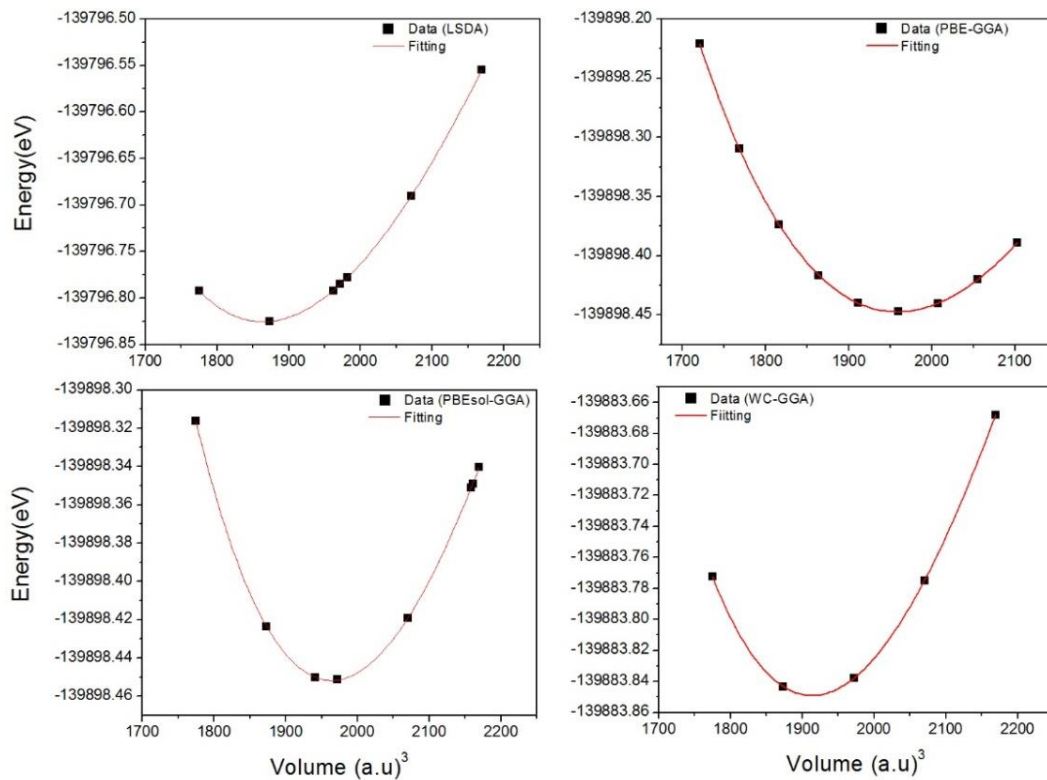


**Figure 1.** Total energy versus unit cell volume by chosen potential for LSTO at room temperature

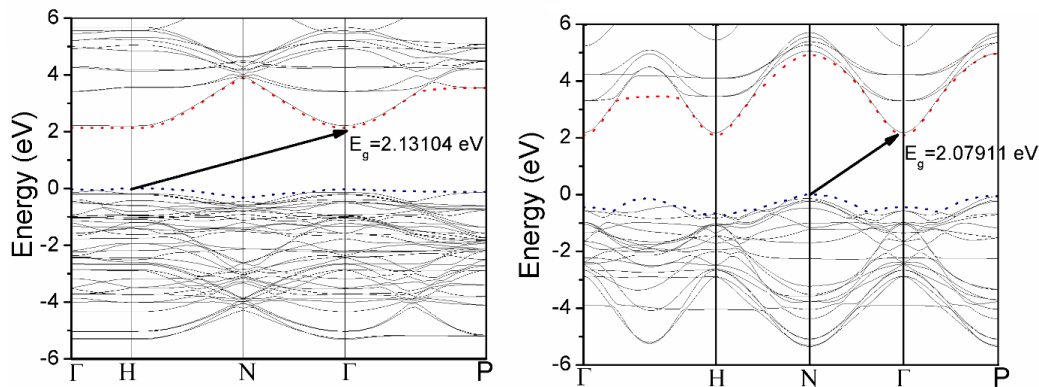
**Table 1.** Calculated ground state lattice constants of LSTO depending chosen pseudo-potential at room temperature

Lattice Constant (Å)	PBE-GGA	LSDA	WC-GGA	PBEsol-GGA	Experimental values[9]
a	18.000	17.273	17.727	18.546	18.182
b	5.785	5.552	5.698	5.961	5.844
c	5.301	274.07	5.441	5.692	5.580

To be consistent for the rest of calculation, PBE-GGA potential was used.

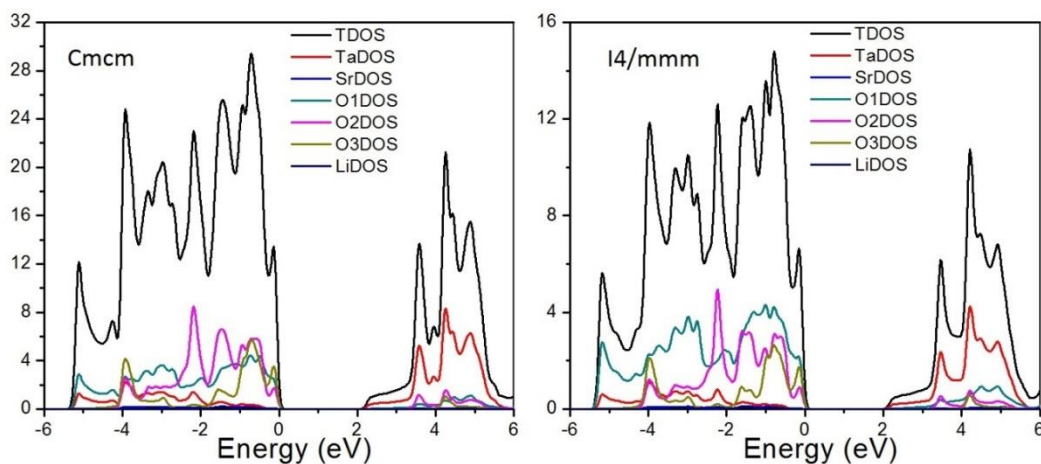
### 3.2. Electronic Properties

Figure 2 shows the top of valence and the bottom of conduction band structure of LSTO in two phases at zero pressure. In general, the band structure of two phases is very similar and has semiconductor character. Forbidden Energy Band Gap value (FEBG) is obtained as a 2,131 eV for Cmc<sub>m</sub> space group at Room Temperature (RT), and 2,079 eV for I4/mmm space group at 300 C. As seen from Figure 2, the separation between valence and conduction band decreases from orthorhombic phase to tetragonal phase. Furthermore, while bottom of the conduction band is located at  $\Gamma$  high symmetry point in the BZ for both phases, top of the valence band is located at H high symmetry point for orthorhombic phase and N high symmetry point for tetragonal phase. In both cases, indirect band transition takes place.



**Figure 2.** Calculated electronic band structure of LSTO for two phases

Materials with wide band gap have technological application areas such as aerospace, power system and high-temperature operations [20]. To compare value FEBG of  $\text{Li}_2\text{CaTa}_2\text{O}_7$  [21] with LSTO, it is seen that the value of FEBG of  $\text{Li}_2\text{CaTa}_2\text{O}_7$  in three phases are higher than LSTO compound in two phases. This is expected situation due to heavier atom of LSTO compound. LSTO compound has Sr element, which is heavier than Ca atom, therefore, it has narrower band gap than  $\text{Li}_2\text{CaTa}_2\text{O}_7$ .



**Figure 3.** Calculated TDOS of LSTO compound for two phases

The electronic density of states (DOS) and the atom resolved partial density of states (PDOS) of LSTO at zero pressure were also shown in Figure 3 for two phases. The semiconductor characteristic is observed firstly. Second observing from DOS is that forbidden energy band gap is getting smaller, from 2,131 eV to 2,079 eV from orthorhombic phase to tetragonal phase. This confirms electronic band structure. However, the partial contribution of atoms has not been changed for two cases. As seen from Figure 3 that Ta atom contributes not only valance band, but also conduction band. The main contribution to valance band comes from O atom regardless of O atom position in structure. Contribution of Li and Sr atoms is ignored comparing with rest of the atoms in compound.

### 3.3. Optical Properties

To explain compound optical properties which is response of material to incoming electromagnetic radiation, the complex dielectric function equation,  $\varepsilon(\omega) = \varepsilon_1(\omega) + i\varepsilon_2(\omega)$ , is used. In the complex dielectric formula,  $\varepsilon_1(\omega)$  related to the electronic polarizability of material represents the real part of the dielectric function,  $\varepsilon_2(\omega)$  associated with the electronic absorption of material is known as the imaginary part. The real and imaginary part of dielectric function  $\varepsilon_1(\omega)$  and  $\varepsilon_2(\omega)$  can be analytically and separately deduced according to Kramers-Kronig transformation [22].

The rest of the optical constant such as the refractive index  $n(\omega)$ , extinction coefficient  $k(\omega)$ , Reflective index  $R(\omega)$  are obtained with real and imaginary parts of the complex dielectric function.

The material structure has to be taken into account, if someone wants to calculate the complex dielectric function of material. LSTO has orthorhombic structure at RT and tetragonal structure at 300 °C, so, all diagonal components of the dielectric tensor depending on axes must be calculated (Figure 4 a-b) at RT and (Figure 5 a-b) at 300 °C.

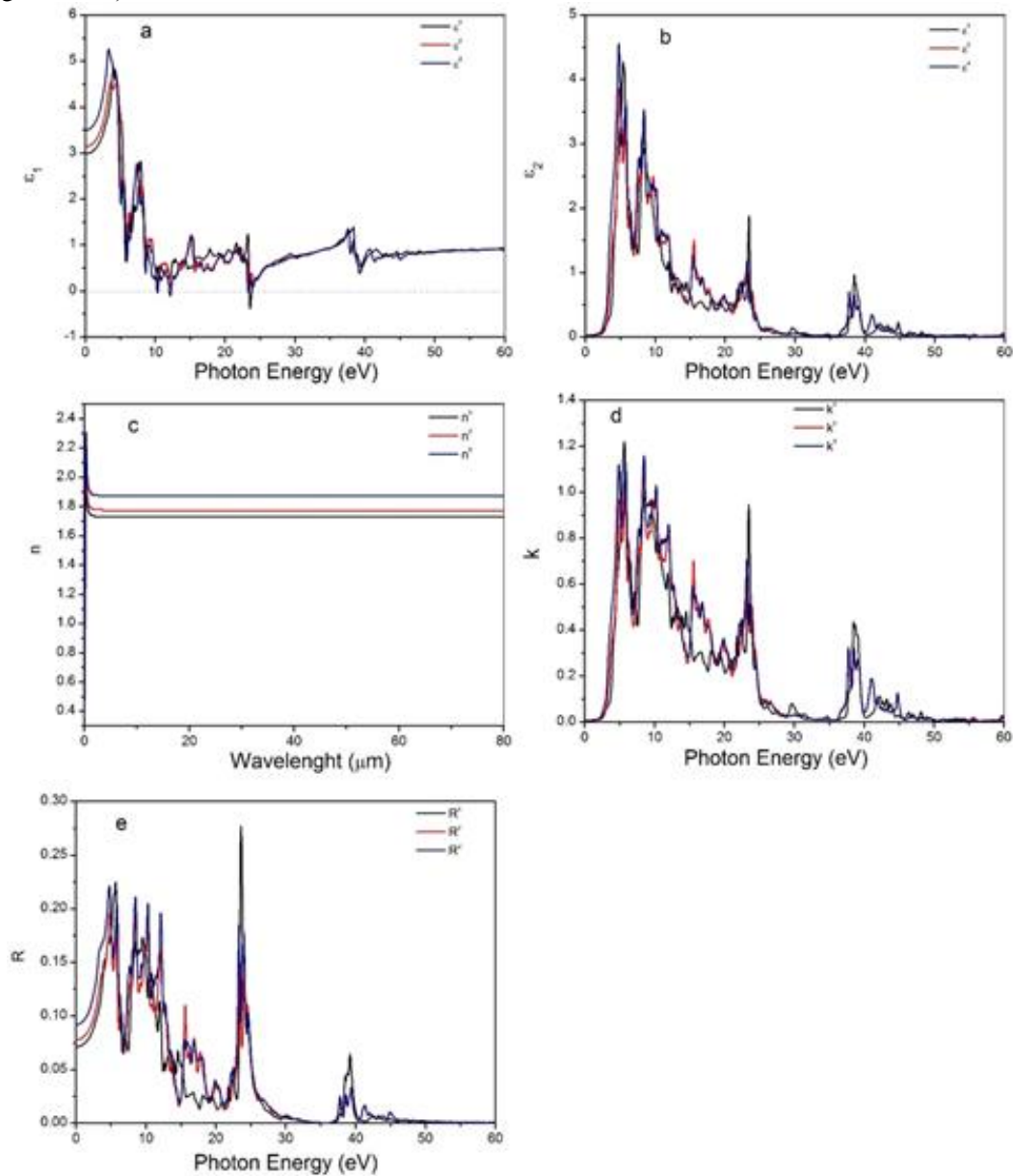


**Figure 4.** Optical constant of LSTO compound axes dependence a) real part and b) imaginary part of dielectric function c) Refractive index d) extinction coefficient e) Reflective index at RT

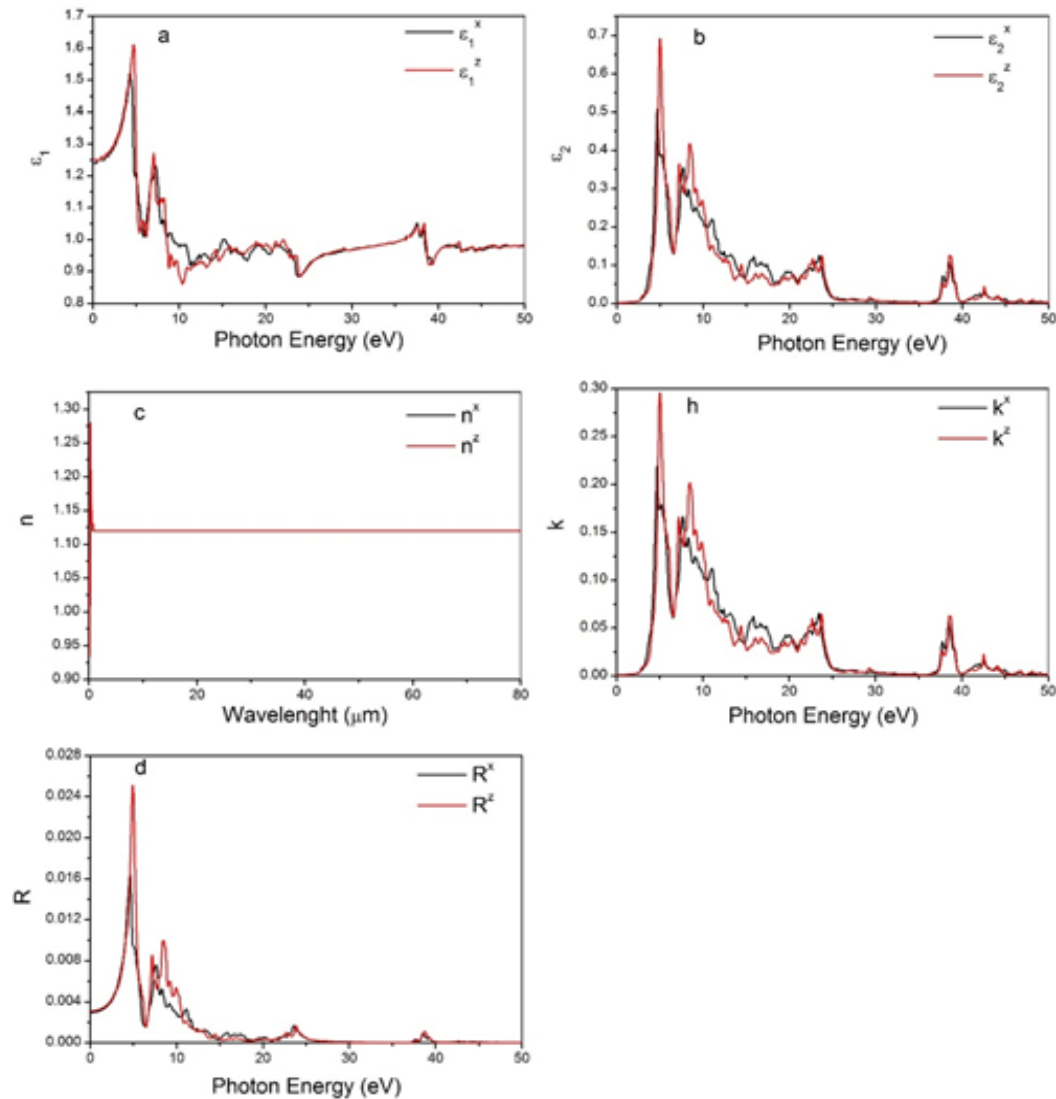


**Figure 5.** Optical constant of LSTO compound axes dependence a) real part and b) imaginary part of dielectric function c) Refractive index d) extinction coefficient e) Reflective index at 300 °C

To understand electronic structure of the dealing compound, the dielectric function is calculated. The  $\epsilon_1(\omega)$  and  $\epsilon_2(\omega)$  components for both LSTO in two phases are plotted in Figures 4 a-b and 5 a-b in the wide range of energy, 0-50 eV. Their similarity is a direct reflection of the density of state for both phases (Figure 3). The major band located around 4 eV is attributed to interband transition from O-2p valence band to Ta-5d conduction band (Figures 4a and 5a).

The dispersion of  $\epsilon_1^x(\epsilon_1^y)$  function of tetragonal phase could be distinguished from  $\epsilon_1^z$  considering anisotropy. Moreover, the anisotropy in the dielectric function, specifically in the range of 8-17 eV, is more pronounced for orthorhombic phase (Figures 4 a b and 5 a b). The static values of the real part of dielectric constant, which are the electronic part, are inserted in Table 2. While the value of  $\epsilon_1^y(0)$  is highest,  $\epsilon_1^x(0)$  has the smallest value at RT. At 300°C, compound undergoes phase transition. Therefore, real part values of complex dielectric function alters,  $\epsilon_1^x(0) = \epsilon_1^y(0) = 1.25$  and  $\epsilon_1^z(0) = 1.24$  (Table 2). Furthermore, at RT, real part of dielectric function goes to negative value between 12-12.5 eV and 23.4-24 eV where compound behaves like metal and reflect all incident electromagnetic light back to coming direction. However, the value of  $\epsilon_1(\omega)$  does not go to negative value at 300 °C.

**Table 2.** Calculated real part of optical dielectric constant, and refractive index of LSTO in two phase

	Room Temperature (Cmcm)	300 °C (I4/mmm)
$\epsilon_1^x(0)$	2.99	1.25
$\epsilon_1^y(0)$	3.14	1.25
$\epsilon_1^z(0)$	3.5	1.24
$n^x(0)$	1.86	1.121
$n^y(0)$	1.77	1.121
$n^z(0)$	1.73	1.122

The imaginary part of the dielectric function has five peaks which are responsible transition from valence band to conduction band (Figure 4b and 5b). Until 2.13 eV at RT and 2.07 eV at 300°C, there is no energy dissipation. After this point, we can see dramatic increasing at 2.13 and 2.07 eV, where transition takes place, at RT and 300 °C, respectively. Broad spectra of the complex dielectric function show high absorption in different regions of the energy spectrum.

The light propagates through the material can be defined by refractive index. The knowledge about refractive index is important quality to use material in the optical devices such as photonic crystal, waveguides, solar cells etc.... Figures 4c and 5c show the refractive index along the crystal axes for RT and 300 C, respectively. Obtained the static values of refractive index depending on interested axis are inserted in Table 2. It is seen from Table 2 or Figures 4c and 5c, refractive index value of selected axes varies. The reason of variation is structural phase transition.

Extinction coefficient is the sum of scattering and absorption, so it represents total effect of medium on radiation passing the medium. Figures 4d and 5d represent extinction coefficient of materials at RT and 300 °C, respectively. First glance indicates similarity between imaginary part of the complex dielectric function and extinction coefficient.

Finally, we plotted the reflectivity versus the energy in Figures 4e and 5e. Carefully and detailed analysis Figures 4e and 5e reveals that 20 % reflection occurs through 5- 12 eV at room temperature, while it ensue at 2 % at 5 eV for 300 °C.

#### 4. CONCLUSION

In summary, the electronic and optical properties of  $\text{Li}_2\text{SrTa}_2\text{O}_7$  in orthorhombic and tetragonal phases were calculated within GGA. The calculated electronic band structure reveals that compound is semiconductor and has indirect band gap. According to density of state graph, while main contribution to conduction band comes from Ta element, contribution of O element is mainly to valence band. Furthermore, optical properties of LSTO are also discussed. Unfortunately, there are a few studies, which focused on synthesized and characterized structure of compound, in literature and none of them have investigated electronic or optical properties of LSTO either experimentally or theoretically. Therefore, we have not made any comparison obtained results with experimental or theoretical data.

#### ACKNOWLEDGEMENTS

This work was supported by the Unit of Scientific Research Projects of VanYuzuncuYil University under project No. FHD-2018-7154.

#### CONFLICTS OF INTEREST

No conflict of interest was declared by the author.

## REFERENCES

- [1] Ruddlesden. S.N., Popper, P., "New compounds of the  $K_2NiF_4$  type", *Acta Crystal*,10, (1957).
- [2] Shimizu, K., Yoshihiro, T., Masato, K., Kenji, T., Tatsuya, K., Mineo, S., and Yoshie, K., "Photocatalytic water splitting over spontaneously hydrated layered tantalate  $A_2SrTa_2O_7 \cdot nH_2O$  (A=H,K,Rb)", *Chemistry Letters*, (11): 1158-1159, (2002).
- [3] Dion, M., Ganne, M., and Tournoux, M., "Mi(an-1nbno $3n+1$ ) Ferroelastic foliated perovskites, where N=2,3 and 4", *Revue De Chimie Minerale*, 23(1): 61-69, (1986).
- [4] Gopalakrishnan, J., and Bhat,V., " $A_2Ln_2Ti_3O_{10}$  (A = K or Rb, Ln = La or Rare-Earth) -A new series of layered perovskites exhibiting ion-exchange", *Inorganic Chemistry*,26(26): 4299-4301, (1987).
- [5] Jacobson, A.J., Johnson,J.W., and Lewandowski, J.T., "Interlayer chemistry between thick transition-metal oxide layers - synthesis and intercalation reactions of  $K[Ca_2Na_n.3Nb_nO_{3n+1}]$  ( $3 \leq n \leq 7$ )", *Inorganic Chemistry*, 24(23): 3727-3729, (1985).
- [6] Toda, K., Kurita, S., and Sato, M., "Synthesis and ionic-conductivity of novel layered perovskite compounds,  $AgLaTiO_4$  and  $AgEuTiO_4$ ", *Solid State Ionics*,81 (3-4): 267-271, (1995).
- [7] Bhuvanesh, N.S.P., Crosnier-Lopez, M.P., Duroy, and H., Fourquet, J. L., "Synthesis and structure of novel layered perovskite oxides:  $Li_2La_{1.78}Nb_{0.66}Ti_{2.34}O_{10}$ , and a new family,  $Li_2[A_{0.5n} B_nO_{3n+1}]$ ", *Journal of Materials Chemistry*, 9(12): 3093-3100, (1999).
- [8] Akbarian-Tefaghi, S., Veiga, E. T., Amand, G., and Wiley, J. B., "Rapid topochemical modification of layered perovskites via microwave reactions", *Inorganic Chemistry*, 55(4): 1604-1612, (2016).
- [9] Pagnier, T., Rosman, N., Galven, C., Suard, E., Fourquet, J. L., Berre, J. L., and Crosnier-Lopez, M. P., "Phase transition in the Ruddlesden-Popper layered perovskite  $Li_2SrTa_2O_7$ ", *Journal of Solid State Chemistry*, 182(2): 317-326, (2009).
- [10] Floros, N., Michel, C., Hervieu, M., and Raveau, B., "New n=2 members of the  $Li_2Sr_{n-1}MnO_{3n+1}$  family, closely related to the Ruddlesden-Popper phases: structure and non-stoichiometry", *Journal of Materials Chemistry*, 9(12): 3101-3106, (1999).
- [11] Schwarz, K., Blaha, P., and Madsen, G.K.H., "Electronic structure calculations of solids using the WIEN2k package for material sciences", *Computer Physics Communications*, 147(1-2): 71-76, (2002).
- [12] Andersen, O.K., "Linear methods in band theory", *Physical Review B*,. 12(8): 3060-3083, (1975).
- [13] Perdew, J.P. and Wang, Y., "Accurate and simple analytic representation of the electron-gas correlation-energy", *Physical Review B*, 45(23): 13244-13249, (1992).
- [14] Perdew, J.P., Burke, K., and Ernzerhof, M., "Generalized gradient approximation made simple", *Physical Review Letters*, 77(18): 3865-3868, (1996).
- [15] Wu, Z.G. and Cohen, R.E., "More accurate generalized gradient approximation for solids", *Physical Review B*, 73(23), (2006).
- [16] Wu, Z.G. and Cohen, R.E., "Reply to "Comment on 'More accurate generalized gradient approximation for solids'", *Physical Review B*, 78(19): (2008).

- [17] Perdew, J.P., Ruzsinszky, A., Csonka, G. I., Vydrov, o. A., Scuseria, G. E., Constantin, L., A., Zhou, X., and Burke, K.,” Restoring the density-gradient expansion for exchange in solids and surfaces”, *Physical Review Letters*, 102(13): (2009).
- [18] Birch, F., “Finite Elastic Strain of Cubic Crystals.” *Physical Review*, 71(11): 809-824, (1947).
- [19] Murnaghan, F.D., “Birch-Murnaghan equation of state”, *Proc Nat. Acad. Sci*, 50:697, (1947).
- [20] Tolbert, L.M., Ozpineci, B., Islam. S., K., and Chinthavali, M., “Wide bandgap semiconductors for utility applications” *IASTED International Conference on Power and Energy Systems (PES2003)*, 317-321, (2003).
- [21] Aycibin, M., “The electronic and optical properties of  $\text{Li}_2\text{SrTa}_2\text{O}_7$  depending on phase transition”, *first international conference on physical chemistry and functional materials, Elazig-Turkey*, (2018).
- [22] Li, Z.L., Xin-You, A., Xin-Lu, C., Xue-Min, W., Hong, Z., Li-Ping, P., and Wei-Dong, W., “First-principles study of the electronic structure and optical properties of cubic Perovskite  $\text{NaMgF}_3$ ”, *Chinese Physics B*, 23(3): (2014).